Available online at www.sciencedirect.com

SciVerse ScienceDirect

Ceramics International 39 (2013) 1163–1167

CERAMICS INTERNATIONAL

www.elsevier.com/locate/ceramint

Magnetic behavior of nickel–bismuth ferrite synthesized by a combined sol–gel/thermal method

Mohammad Javad Nasr Isfahani[a,*,1], Marjaneh Jafari Fesharaki[b], Vladimir Šepelák[c]

[a]Department of Physics, Lenjan Branch, Islamic Azad University, Isfahan, Iran
[b]Department of Physics, Faculty of Science, Payame Noor University, Zarinshahr 74718-191, Iran
[c]Institute of Nanotechnology, Karlsruhe Institute of Technology, Herrmann-von-Helmholtz-Platz 1, 76344 Eggenstein-Leopoldshafen, Germany

Received 23 March 2012; received in revised form 10 July 2012; accepted 10 July 2012
Available online 27 July 2012

Abstract

The bulk $NiFe_{2-x}Bi_xO_4$ ferrites with various Bi^{3+} concentration ($x=0$, 0.1, 0.15) were synthesized via sol–gel procedure, starting from nickel, bismuth and iron nitrate powders, followed by the conventional thermal treatment. The structural and magnetic properties of the as-prepared ferrites were studied by means of X-ray diffraction, alternating gradient force magnetometry and Faraday balance. The anisotropy constant was determined by the law of approach to saturation (LAS) model. An increasing Bi^{3+} concentration in $NiFe_{2-x}Bi_xO_4$ leads to a decrease in the saturation magnetization, Néel temperature and the anisotropy constant of the material.

Keywords: Nickel–bismuth ferrite; Combined sol–gel/thermal synthesis; Magnetic behavior; Anisotropy constant

1. Introduction

Ferrites with the spinel structure of the type MFe_2O_4 (M is a divalent cation) are magnetic ceramics of great importance [1]. Their applications range from simple function devices to sophisticated devices for electronics. Some interesting applications are in computer peripherals, telecommunication equipments, electronic and microwave devices, magnetic media, recording devices and magnetic cards. It is well recognized that electrical and magnetic properties of spinel ferrites depend on various parameters such as their processing conditions and chemical composition [1–4]. These complex oxides crystallize in an *fcc* structure with the transition metal cations (M^{2+}, Fe^{3+}) residing at the interstices formed by oxygen anions. To emphasize the site occupancy at the atomic level, the structural formula of spinel ferrites may be written as $(M^{2+}_{1-\lambda}Fe^{3+}_{\lambda})[M^{2+}_{\lambda}Fe^{3+}_{2-\lambda}]O_4$, where parentheses and square brackets denote cation sites of tetrahedral (A) and octahedral [B] coordinations, respectively. λ represents the degree of inversion defined as the fraction of the (A) sites occupied by Fe^{3+} cations.

Nickel ferrite, $NiFe_2O_4$, as a soft magnetic n-type semiconducting material, is an important member of the spinel family with a fully inverse structure ($\lambda=1$) in the bulk state [5,6]. It has been revealed that an increase in temperature and the particle size reduction of a spinel induce the cation redistribution that is directed towards random arrangement [7]. In both, undoped and substituted forms, $NiFe_2O_4$ serves as a material for high-frequency applications in telecommunication field. Due to its high resistivity and low eddy current losses it is used in radio-frequency circuits, high quality filters, rod antennas, transformer cores, read/write heads for high-speed digital tape and operating devices [8].

In previous paper [9], we reported structural and magnetic properties of $NiFe_{2-x}Bi_xO_4$ nanoparticles prepared via sol–gel method. The present work represents a continuation of our work [9] with the goal to characterize the bulk $NiFe_{2-x}Bi_xO_4$ ($x=0$, 0.1, and 0.15) synthesized by the combined sol–gel/thermal method. Crystal structure and magnetic properties (Néel temperature, saturation magnetization and anisotropy constant) of the as-prepared bulk samples are investigated as a function of Bi^{3+} concentration, and are

*Corresponding author. Tel.: +98 9133195944; fax: +98 3342432409.
E-mail address: m.nasr@iauln.ac.ir (M.J. Nasr Isfahani).
[1]This work is dedicated to my wife Ghazale.

0272-8842/$ - see front matter © 2012 Elsevier Ltd and Techna Group S.r.l. All rights reserved.
http://dx.doi.org/10.1016/j.ceramint.2012.07.040

compared with those of $NiFe_{2-x}Bi_xO_4$ nanoparticles. Note that although a lot of work concerning the substituted nickel ferrites has already been published, see, e.g. [4,9–18], to the best of our knowledge, there is no report in the literature on $NiFe_{2-x}Bi_xO_4$ prepared via sol–gel procedure followed by the thermal treatment.

2. Experimental

Nickel–bismuth ferrites, $NiFe_{2-x}Bi_xO_4$ with $x=0$, 0.1, and 0.15, were synthesized in the bulk form by the combined sol–gel/thermal method. At first, stoichoimetric amounts of $Fe(NO_3)_3$, $Ni(NO_3)_2$ and $Bi(NO_3)_3$ were dissolved completely in deionized water. In the dissolving process, the molar ratio of cation concentrations of $Ni^{2+}/(Bi^{3+}+Fe^{3+})$ was fixed at 1:2 and that of $xBi^{3+}/(2-x)Fe^{3+}$ was varied with $x=0$, 0.1 and 0.15. Each aqueous solution containing Ni^{2+}, Fe^{3+} and Bi^{3+} was poured into citric acid with the ratio of $(Ni^{2+}+Bi^{3+}+Fe^{3+})/(\text{citric acid})=3$. The mixtures were stirred and slowly evaporated at 353 K to form gels. These gels were dried at 373 K for 2 h and then annealed in air at 1273 K for 3 h.

The structure of the as-prepared $NiFe_{2-x}Bi_xO_4$ was studied using an X-ray diffractometer (D8, Bruker, Germany) with CuKα radiation ($\lambda_{Cu}=1.54056$ Å). The Néel temperature and the hysteresis (M–H) loops of the samples were measured by a Faraday balance equipped with a permanent magnet (0.02 T) and an alternating gradient force magnetometer (AGFM), respectively.

3. Results and discussion

The XRD patterns of the as-prepared nickel–bismuth ferrites with various Bi^{3+} concentration ($x=0$, 0.1, and 0.15) are shown in Fig. 1. The diffraction patterns of the samples confirm that the spinel phase was formed. It is clearly seen that the diffraction lines for all three samples are relatively narrow, indicating their polycrystalline (bulk) character. The lattice parameters of the cubic ferrites, a, is calculated using the following formula [19]:

$$a=\frac{\lambda_{Cu}\sqrt{h^2+k^2+l^2}}{2\sin\theta} \quad (1)$$

where θ is the Bragg angle and h, k and l are the Miller indices. Variation of the lattice parameter of the ferrites with Bi^{3+} concentration is presented in Fig. 2. As clearly visible, the lattice parameter of $NiFe_{2-x}Bi_xO_4$ samples increases with increasing Bi^{3+} concentration. This can be attributed to the different sizes of Bi^{3+} and Fe^{3+} ions; Bi^{3+} has larger ionic radius (1.31 Å) than Fe^{3+} ions (0.66 Å) [20].

From the determined a values, X-ray density (d_x) of the Bi-substituted nickel ferrites was calculated using the following formula [19]:

$$d_x=\frac{8M}{Na^3} \quad (2)$$

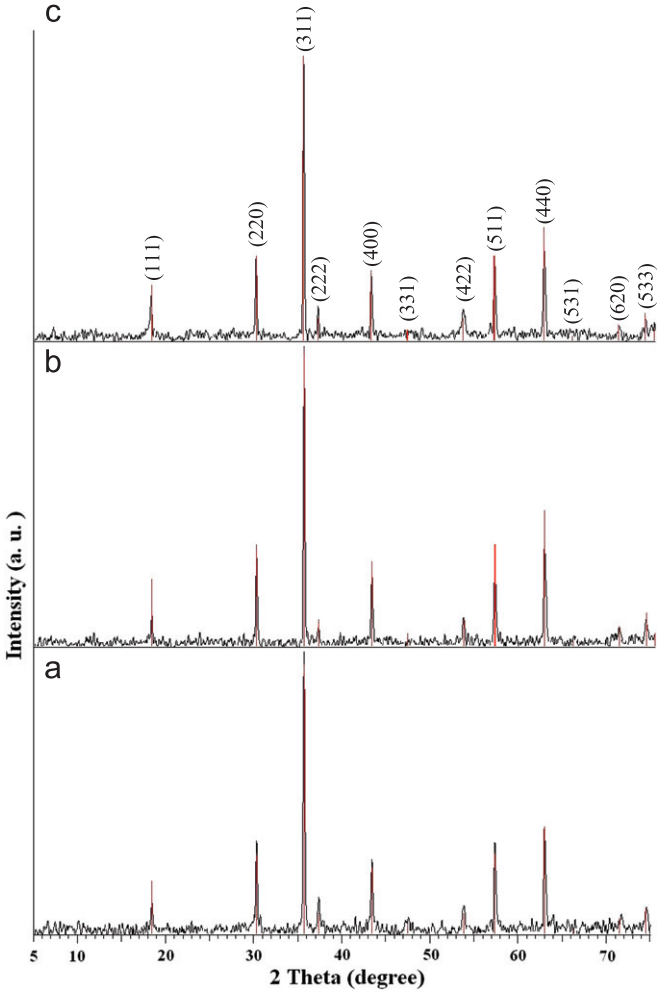

Fig. 1. XRD patterns of polycrystalline $NiFe_{2-x}Bi_xO_4$ samples: (a) $x=0$, (b) $x=0.1$, (c) $x=0.15$, prepared by the thermal treatment of $NiFe_{2-x}Bi_xO_4$ nanoparticles synthesized by the sol–gel procedure. The diffraction peaks are denoted by Miller indices corresponding to the spinel phase (JCPDS PDF 10-0325).

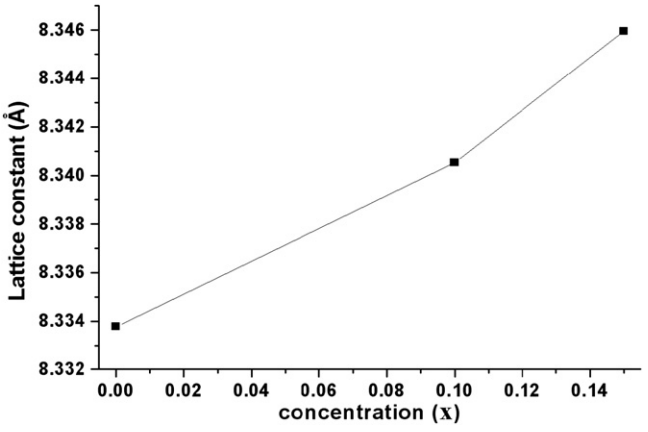

Fig. 2. Variation of the lattice parameter of $NiFe_{2-x}Bi_xO_4$ with Bi content.

where M and N are the molecular weight and Avogadro's number, respectively. The d_x values are presented in Table 1 and Fig. 3, indicating the increase of X-ray density of $NiFe_{2-x}Bi_xO_4$ with increasing Bi^{3+}.

Table 1
The structural and magnetic characteristics (lattice parameter, a, X-ray density, d_x, saturation magnetization, M_s, Néel temperature, T_N, and the anisotropy constant, K_1) of $NiFe_{2-x}Bi_xO_4$ ($x=0$, 0.1, 0.15) samples. The M_s values of the as-prepared bulk ferrites are compared with those of the corresponding nanocrystalline $NiFe_{2-x}Bi_xO_4$ counterparts [9].

x	a (Å)	d_x (g cm^{-3})	M_s (emu g^{-1})	M_s (emu g^{-1})[a]	T_N (K)	K_1 (erg cm^{-3})
0	8.334	5.379	44	42	848	76723
0.1	8.341	5.716	40	35	788	51547
0.15	8.346	5.881	38	29	753	50284

[a]Data taken from Ref. [9].

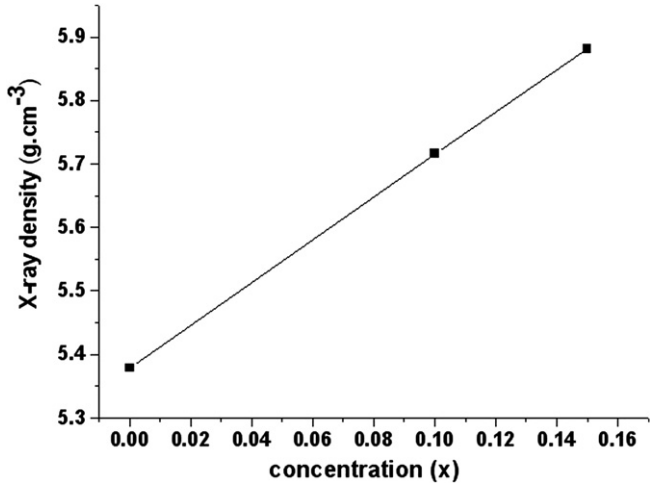

Fig. 3. The X-ray density of $NiFe_{2-x}Bi_xO_4$ versus Bi content (x).

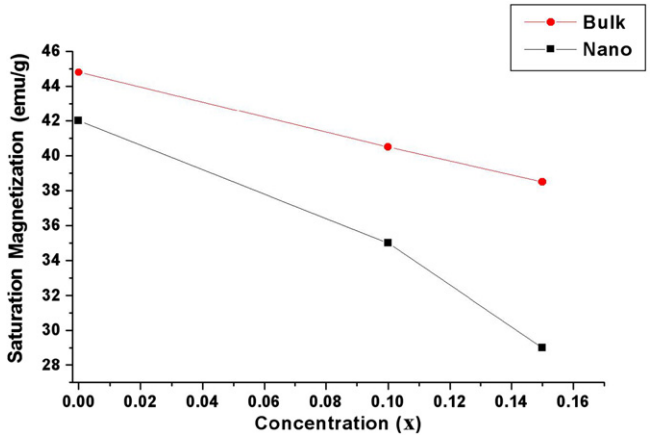

Fig. 5. Magnetization of bulk and nanocrystalline $NiFe_{2-x}Bi_xO_4$ samples versus x. The M_s values of nanocrystalline $NiFe_{2-x}Bi_xO_4$ are taken from Ref. 9.

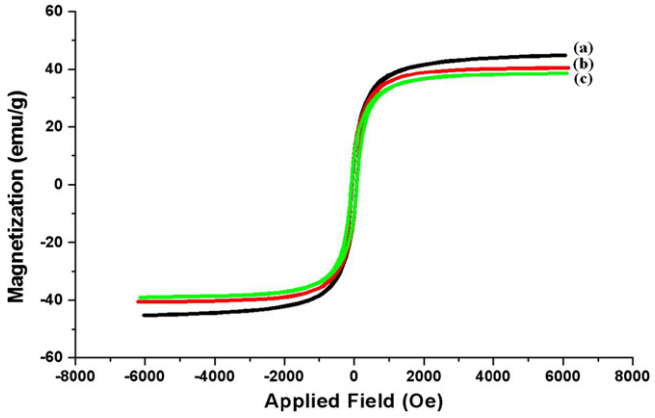

Fig. 4. The hysteresis loops for $NiFe_{2-x}Bi_xO_4$ samples: (a) $x=0$, (b) $x=0.1$, (c) $x=0.15$, recorded at room temperature.

Fig. 4 shows the hysteresis curves of the $NiFe_{2-x}Bi_xO_4$ ($x=0$, 0.1, 0.15) samples. The measured values of the saturation magnetization (M_s) for all the samples are presented in Table 1, indicating the decrease of M_s with increasing Bi^{3+} concentration. This behavior is explained by the magnetic dilution of the ferrite system with nonmagnetic Bi^{3+} ions; i.e., in the present case, an Fe^{3+} ion with an effective magnetic moment of 5 μ_B is substituted by a nonmagnetic Bi^{3+} cation. Note that a very small hysteresis for all the as-prepared samples indicates that the Ni–Bi ferrite can be used most efficiently as a soft magnetic material with a negligible hysteresis loss [21]. From the qualitative point of view, these results are similar to those reported in our work for nanocrystalline Ni–Bi ferrite prepared via the sol–gel method [9]. Quantitatively, the saturation magnetization for the bulk $NiFe_{2-x}Bi_xO_4$ samples is significantly greater than that of corresponding nanocrystalline counterparts, see Fig. 5. As it is generally accepted, a reduction of the saturation magnetization with decreasing size of ferrite particles can be attributed to the presence of canted spins and nonequilibrium cation distribution in the surface shell of nanoparticles [3,6,22,23].

The temperature-dependent magnetic measurements (Fig. 6) revealed that the Néel temperature (T_N) of the as-prepared $NiFe_{2-x}Bi_xO_4$ shifts towards lower temperature with increasing Bi^{3+} concentration; $T_N=848$, 788 and 753 K for $x=0$, 0.1 and 0.15, respectively. The Néel temperature of a ferrimagnetic spinel oxide has been found to be closely related to the number of Fe^{3+}(A)–O^{2-}–Fe^{3+}[B] linkages per formula unit of a material and also to the distribution of Fe^{3+} ions over the (A) and [B] sites [24]. Thus, the observed reduction of T_N with increasing x in $NiFe_{2-x}Bi_xO_4$ may be interpreted as a consequence of weakening of the (A)–[B] superexchange interaction due to

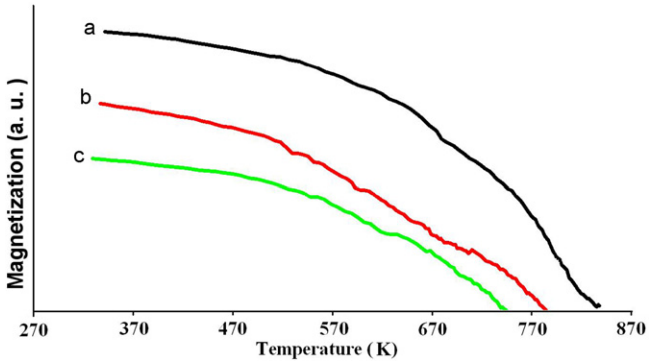

Fig. 6. The temperature-dependent magnetization for $NiFe_{2-x}Bi_xO_4$ samples: (a) $x=0$, (b) $x=0.1$, (c) $x=0.15$, recorded at $H=0.002$ T.

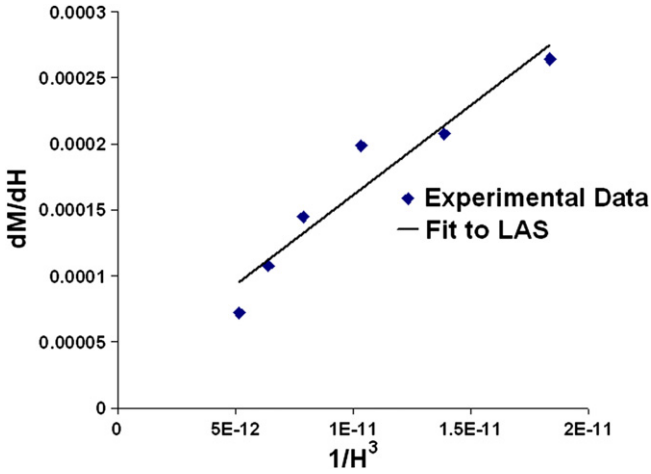

Fig. 7. Magnetization data for $NiFe_{1.9}Bi_{0.1}O_4$ fitted using the LAS model.

the substitution of the Fe^{3+} ions by nonmagnetic Bi^{3+} cations. In such a case, the internal energy required to offset the spin alignment will decrease and the Néel temperature is expected to fall.

The anisotropy constant for the $NiFe_{2-x}Bi_xO_4$ samples ($x=0$, 0.1, 0.15) was estimated using the "Law of approach to saturation (LAS)" model [24]. According to this theory, the dependence of magnetization, M, on the applied magnetic field, H, is given by

$$M = M_s[1-(b/H^2)]+kH \quad (3)$$

where $b=(8/105)$ $(K_1^2/\mu_0^2 M_s^2)$, μ_0 is the permeability of the free space, K_1 is the cubic anisotropy constant and the term kH is known as the forced magnetization. Note that the forced magnetization causes a linear increase in the spontaneous magnetization especially at high fields. The numerical coefficient 8/105 applies to cubic anisotropy of random polycrystalline samples. In the present series, the experimental data [M–H curve] above 0.5 T (high field parts) are fitted to Eq. (3) (with the fitting parameters M_s and K_1) neglecting the forced magnetization term. A typical curve (straight line) fitted to LAS is shown in Fig. 7 for the sample $NiFe_{1.9}Bi_{0.1}O_4$. The anisotropy

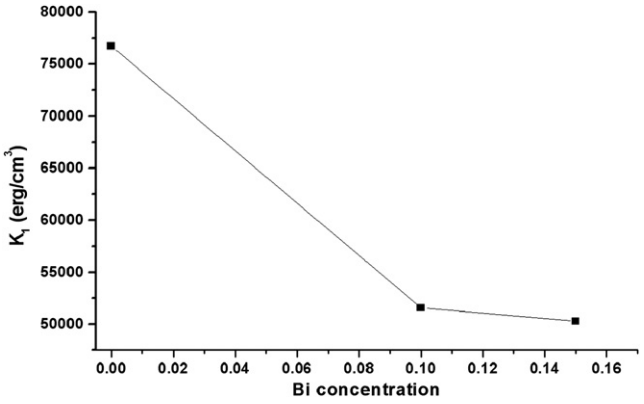

Fig. 8. Variation of the cubic anisotropy constant with x for $NiFe_{2-x}Bi_xO_4$.

constants of the $NiFe_{2-x}Bi_xO_4$ samples ($x=0$, 0.1 and 0.15) with various Bi^{3+} concentrations are shown in Fig. 8. As it is seen, an increasing Bi^{3+} concentration leads to a decrease in the anisotropy constant. In pure $NiFe_2O_4$, the Fe^{3+} ions occupy both (A) and [B] sites; thus the strong anisotropy is primarily due to the presence of Fe^{3+} ions on the octahedral sites of the spinel structure. The crystal field (trigonal field) is not capable of removing the orbital degeneracy of Fe^{3+} ions at the octahedral sites so that the orbital magnetic moment is not quenched and therefore there is a strong spin–orbit coupling, which produces large magnetocrystalline anisotropy energy. The substitution of Fe^{3+} ions by Bi^{3+} cations on [B] sites in $NiFe_{2-x}Bi_xO_4$ [9] reduces the spin–orbit coupling, which may lead to a decrease in the anisotropy constant of the substituted ferrites.

4. Conclusions

Nickel–bismuth ferrites in the bulk form with various Bi^{3+} concentrations ($x=0$, 0.1, 0.15) were synthesized by the thermal treatment of $NiFe_{2-x}Bi_xO_4$ nanoparticles previously prepared by sol–gel technique. The lattice parameter of the as-prepared cubic ferrites increases with increasing x due to the larger ionic radius of Bi^{3+} in comparison to that of Fe^{3+} ions. The decrease in the saturation magnetization and Néel temperature of the samples with increasing Bi^{3+} concentration is explained by the effect of magnetic dilution of the ferrite system and, consequently, by the weakening of the (A)–[B] super-exchange interaction, respectively. The substitution of the magnetic Fe^{3+} ions by nonmagnetic Bi^{3+} cations reduces the spin–orbit coupling leading to a decrease in the anisotropy constant of the ferrites. The Bi-substituted nickel ferrites exhibit a soft magnetic behavior.

Acknowledgments

The authors thank Mr. A. Pourmoghaddas (Carleton University, Ottawa, Canada) for his helpful discussions and Mr. M. Alikhani (Kashan University, Kashan, Iran) for the AGFM measurements. The XRD patterns were

measured at the Central Laboratory of the Isfahan University.

References

[1] M.J. Nasr Isfahani, M. Myndyk, V. Šepelák, J. Amighian, A Mössbauer effect investigation of the formation of MnZn nanoferrite phase, Journal of Alloys and Compounds 470 (2009) 434.

[2] M.J. Nasr Isfahani, M. Myndyk, D. Menzel, A. Feldhoff, J. Amighian, V. Šepelák, Magnetic properties of nanostructured MnZn ferrite, Journal of Magnetism and Magnetic Materials 321 (2009) 152.

[3] V. Šepelák, A. Feldhoff, P. Heitjans, F. Krumeich, D. Menzel, F.J. Litterst, I. Bergmann, K.D. Becker, Nonequilibrium cation distribution, canted spin arrangement, and enhanced magnetization in nanosized $MgFe_2O_4$ prepared by a one-step mechanochemical route, Chemistry of Materials 18 (2006) 3057.

[4] M.Eghbali Arani, M.J. Nasr Isfahani, M.Almasi Kashi, Preparation and magnetic studies of nickel ferrite nanoparticles substituted by Sn^{4+} and Cu^{2+}, Journal of Magnetism and Magnetic Materials 322 (2010) 2944.

[5] G. Nabiyouni, M.Jafari Fesharaki, M. Mozafari, J. Amighian, Characterization and magnetic properties of nickel ferrite nanoparticles, Chinese Physics Letters 27 (2010) 126401.

[6] V. Šepelák, I. Bergmann, A. Feldhoff, P. Heitjans, F. Krumeich, D. Menzel, F.J. Litterst, S.J. Campbell, K.D. Becker, Nanocrystalline nickel ferrite, $NiFe_2O_4$: mechanosynthesis, nonequilibrium cation distribution, canted spin arrangement, and magnetic behavior, Journal of Physical Chemistry C 111 (2007) 5026.

[7] V. Šepelák, K.D. Becker, Comparison of the cation inversion parameter of the nanoscale milled spinel ferrites with that of the quenched bulk materials, Materials Science and Engineering A 375–377 (2004) 861.

[8] A. Goldman, Modern Ferrite Technology, Springer, New York, 2006.

[9] M.J. Nasr Isfahani, P. Nasr Isfahani, K.L. Da Silva, A. Feldhoff, V. Šepelák, Structural and magnetic properties of $NiFe_{2-x}Bi_xO_4$ ($x=0$, 0.1, 0.15) nanoparticles prepared via sol–gel method, Ceramics International 37 (2011) 1905.

[10] M.J. Nasr Isfahani, M. Myndyk, M. Eghbali Arani, J. Šubrt, V. Šepelák, Structural and magnetic properties of $NiFe_{2-2x}Sn_xCu_xO_4$, Journal of Magnetism and Magnetic Materials 322 (2010) 1744.

[11] N. Ponpandian, A. Narayanasamy, C.N. Chinnasamy, N. Sivakumar, J.M. Greneche, K. Chattopadhyay, K. Shinoda, B. Jeyadevan, K. Tohji, Néel temperature enhancement in nanostructure nickel zinc ferrite, Applied Physics Letters 86 (2005) 192510.

[12] B.K. Labde, M.C. Sable, N.R. Shamkuwar, Structural and infra-red studies of $Ni_{1+x}Pb_xFe_{2-2x}O_4$ system, Materials Letters 57 (2003) 1651.

[13] K.M. Batoo, S. Kumar, C.G. Lee, Finite size effect and influence of temperature on electrical properties of nanocrystalline Ni–Cd ferrites, Current Applied Physics 9 (2009) 1072.

[14] A.C.F.M. Costa, M.R. Morelli, R.H.G.A. Kiminami, Microstructure and magnetic properties of $Ni_{1-x}Zn_xFe_2O_4$ synthesized by combustion reaction, Journal of Materials Science 42 (2007) 779.

[15] C.M. Liu, L.M. Fang, X.T. Zu, W.L. Zhou, The magnetism and photoluminescence of nickel-doped SnO_2 nano-powders, Physica Scripta 80 (2009) 065703.

[16] A. Azizi, S.K. Sadrnezhaad, Effects of annealing on phase evolution, microstructure and magnetic properties of mechanically synthesized nickel-ferrite, Ceramics International 36 (2010) 2241.

[17] P.P. Sarangi, S.R. Vadera, M.K. Patra, N.N. Ghosh, Synthesis and characterization of pure single phase Ni–Zn ferrite nanopowders by oxalate based precursor method, Powder Technology 203 (2010) 348.

[18] M. Al-Haj, Microstructure characterization and magnetic behavior of $NiAl_xFe_{2-x}O_4$ and $Ni_{1-y}Mn_yAl_{0.2}Fe_{1.8}O_4$ ferrites, Journal of Magnetism and Magnetic Materials 311 (2007) 517.

[19] B.D. Cullity, Elements of X-ray Diffraction, Addison-Wesley Publishing, Reading, MA, 1956.

[20] J. Smit, Magnetic Properties of Materials, McGraw Hill Book Co., 1971.

[21] B.D. Cullity, Introduction to Magnetic Materials, Addison-Wesley Publishing, Reading, MA, 2001.

[22] C. Rath, S. Anand, R.P. Das, K.K. Sahu, S.D. Kulkarini, S.K. Date, N.C. Mishra, Dependence on cation distribution of particle size, lattice parameter, and magnetic properties in nanosized Mn-Zn ferrite, Journal of Applied Physics 91 (2002) 2211.

[23] R.H. Kodama, A.E. Berkowitz, E.J. McNiff, S. Foner, Surface spin disorder in $NiFe_2O_4$ nanoparticles, Physical Review Letters 77 (1996) 394.

[24] S. Chikazumi, Physics of Ferromagnetism, second ed., Oxford University Press, New York, 1997.